Analysis of the Contribution of Cardiovascular Compartments to the Ballistocardiogram Signal Using Mathematical Modeling

Mohamed Zaid, Raul Invernizzi, Lorenzo Sala, Laurel A. Despins, Mihail Popescu, Marjorie Skubic, James Keller, Riccardo Sacco, Marcela Szopos, Virginia H. Huxley, et al.

HAL Id: hal-04275292

https://hal.inrae.fr/hal-04275292v1

Submitted on 9 Jan 2024

Analysis of the Contribution of Cardiovascular Compartments to the Ballistocardiogram Signal Using Mathematical Modeling

Mohamed Zaid[1], Raul Invernizzi[2], Lorenzo Sala[3], Laurel Despins[4], Mihail Popescu[5], James Keller[6], Marjorie Skubic[6], Riccardo Sacco[2], Marcela Szopos[7], Virginia H. Huxley[8], Giovanna Guidoboni[1]

[1] Maine College of Engineering and Computing, University of Maine, Orono ME, USA
[2] Department of Mathematics, Politecnico Di Milano, Milan, Italy
[3] INRAE, MaIAGE, Universite Paris-Saclay, Paris, France
[4] Sinclair School of Nursing, University of Missouri, Columbia MO, USA
[5] Health Management and Informatics, University of Missouri, Columbia MO, USA
[6] Electrical and Computer Engineering, University of Missouri, Columbia MO, USA
[7] Université Paris Cité, CNRS, MAP5, F-75006 Paris, France
[8] Department of Medical Pharmacology and Physiology, University of Missouri, Columbia MO, USA

Abstract

The ballistocardiogram (BCG) captures the mechanics and fluid-dynamic properties of the cardiovascular system and provides useful insights into cardiovascular function. However, the cardiovascular mechanisms generating the BCG are still poorly understood and this limits its clinical applications. The present work examines computer-aided methods for understanding the cardiovascular foundations of the BCG signal. The main goal is to investigate how different cardiovascular compartments contribute to the BCG waveform. This is achieved by comparing BCG signals generated by cardiovascular models of increased complexity, while assessing the impact on pressure-volume loops in the left ventricle. All models describe the circulation as a closed-loop system, which is crucial to capture the dynamic interplay among all cardiovascular compartments, with increasing anatomical and physiological detail. The results highlight the importance of including the ventricles, the main arteries, and the cerebral vasculature in a constructive model for the BCG. The findings emphasize the potential of mathematical modeling to significantly impact cardiovascular diagnostics and healthcare.

1. Introduction

The ballistocardiogram (BCG) is a physiological signal generated by the repetitive motion of the center of mass of the human body as the blood moves within the circulatory system at each heartbeat [1]. The BCG offers a more comprehensive assessment of cardiovascular performance than conventional monitoring techniques, since it captures the mechanical and fluid-dynamical characteristics of the cardiovascular system as a whole. While having the great advantage of being acquired non-invasively, the use of BCG as a clinical monitoring and diagnostic tool is limited by the scarce understanding of the cardiovascular mechanisms responsible for changes in the signal. Computer-aided approaches can help provide a mechanistic and quantitative interpretation of BCG signals, as pioneered by Starr and Noordergraaf and further developed by various research groups [1–5]. In particular, the present study aims to understand the influence of various vascular compartments on the model-predicted BCG waveform. Mathematical models of the cardiovascular system of increasing levels of complexity are considered and the corresponding simulated BCG signals are compared. In [6], changes in BCG signals have been connected to changes in the left ventricle (LV) pressure-volume (PV) loops, which provide quantitative information about the contractile state of the heart. Therefore, this study also considers the model-generated PV loops when comparing the predictions across the hierarchy of cardiovascular models. Ultimately, the goal is to advance the understanding of BCG signals based on cardiovascular mechanisms and aid their potential clinical uses in cardiovascular monitoring.

2. Methods

2.1. Cardiovascular Closed-Loop Models

The starting point for the hierarchy of models considered in this work is the closed-loop system proposed by Avanzolini et al [7], henceforth referred to as Model 0.

The model includes the left and right ventricles along with a lumped description of the systemic and pulmonary circulations. The hierarchy of models summarized in Table 1 embodies a progressively more detailed description of the large arteries (aorta, iliac arteries) and of the cerebral circulation, till reaching the complexity of Model 5, which was introduced by Guidoboni et al in [5].

Table 1. Summary of the features of the hierarchy of cardiovascular closed-loop models considered in this work.

Model type	Heart LV+RV	Pulmonary circulation	Systemic circulation							Cerebral circulation
			Asc	Arc	Thor	Abd	Iliac	Body	
Model 0 (Avanzolini, et al.)	✔	✔						✓	✗
Model 1	✔	✔	Group 1			Group 2		✓	✗
Model 2	✔	✔	✓	✓	✓	Group 3		✓	✗
Model 3	✔	✔	Group 1			Group 2		✓	✔
Model 4	✔	✔	✓	✓	✓	Group 3		✓	✔
Model 5 (Guidoboni, et al.)	✔	✔	✓	✓	✓	✓	✓	✓	✔

2.2. Model-generated BCG waveform

The pioneering work of Starr and Noordergraaf paved the way for a theoretical foundation to interpret the BCG [1]. The force generated by the BCG is a function of the blood volumes occupying different vascular compartments at a given time during the cardiac cycle. Considering the head-to-toe direction and denoting the force as $f_{BCG}(t)$, this can be written as

$$f_{BCG}(t) = M \cdot a_{BCG} = \rho_b \sum_{i=1}^{N} \frac{d^2 V_i(t)}{dt^2} y_i(t)$$

where M is the mass of the subject, ρ_b is the blood density, N is the total number of vascular compartments under consideration, $V_i(t)$ is the blood volume filling the compartment i at the time t, and $y_i(t)$ is the head-to-toe coordinate of the compartment i with respect to the heart plane.

The total number of vascular compartments N differs among the closed-loop models described in Section 2.1, where N increases with model complexity. Specifically, N goes from 4 in Model 0 to 9 in Model 5. This direct connection between model complexity and BCG waveform allows us to investigate what is the minimal complexity that is necessary to capture essential BCG features.

2.3. Model-generated LV-PV loops

Each closed-loop model described in Section 2.1 shares the same mathematical representation for the left ventricle (LV), which originates from the electric analogy to fluid flow reported in Fig. 1. The LV volume corresponds to the electric charge that accumulates on the nonlinear capacitor

described by the time-varying elastance E_L. The LV pressure corresponds to the electric potential in the node LV circled. Thus, by applying Kirchhoff's laws to the electrical circuits representing each model in the hierarchy, it is possible to obtain the LV-PV loop as part of the numerical solution. The activation function, $a(t)$, employed for the pumping timing of the heart is the same for each model. It is a modified version of the original $a(t)$ proposed in [7]:

$$a(t) = \begin{cases} \frac{1}{2} \left[\tanh(q_{L/R}\, t_a) - \tanh(q_{L/R}\, t_b) \right] & \text{if } t_m < T_s \\ 0 & \text{if } t_m \geq T_s \end{cases}$$

where T_s is the time duration of the systole, $q_{L/R}$ is a frequency parameter, t_a and t_b are time parameters [5].
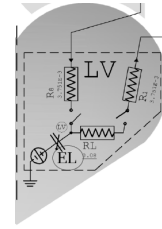

Figure 1. Electrical analogy of left ventricular blood flow.

3. Results and Discussion

A typical BCG waveform is characterized by the so-called I, J, K, L, M, and N peaks and valleys [1]. LV-PV loops typically exhibit four phases (filling, isovolumetric contraction, ejection, isovolumetric relaxation), with volumes and pressures typically in the range 40-170 ml and 2-120 mmHg, respectively [8,9]. The BCG waveforms and LV-PV loops simulated over a cardiac cycle using the six models summarized in Table 1 are reported in Figures 2 and 3. The BCG and LV-PV loop generated by Model 5 (Fig. 2-3, black) have been validated against clinical and experimental data [6] and will be used as reference for comparison with the other models.

MODEL 0: Although Model 0 gives a fundamental understanding of cardiovascular relationships, its simplicity does not appear to be detailed enough to capture essential features of the BCG waveform, which only exhibits the L peak (Fig. 2, red). The LV-PV loop shape is reasonable, but the values of volume and pressure are on the high end of physiological ranges (Fig. 3, red). These results are not unexpected, since Model 0 does not contain an extensive description of the main arteries and, consequently, the dynamic effect of fluid volume in them does not explicitly contribute to the BCG.

MODEL 1: The BCG signal (Fig. 2, blue) exhibits a remarkable improvement in shape when compared to what is produced by Model 0. Typical BCG peaks and valleys become more apparent, even though they are delayed in time
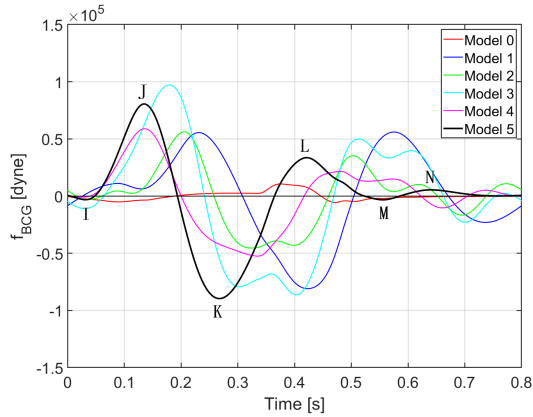
Figure 2. BCG waveform in the head-to-toe direction, f_{BCG}, simulated over one cardiac cycle for each closed-loop cardiovascular model. The BCG simulated using Model 5 exhibits the I, J, K, L, M, and N peaks and valleys that characterize experimental BCG signals.
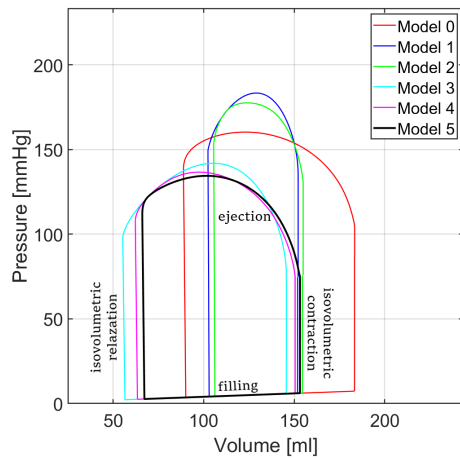

Figure 3. Left ventricular pressure-volume loops simulated over one cardiac cycle for each cardiovascular model.

with respect to what is predicted by Model 5. In addition, the J peak is not as prominent, since its amplitude is similar to that of the L peak. This improvement in the BCG indicates that the waveform benefits from the addition of a more detailed description of the large arteries, which are modeled as two major Groups (Fig. 4). The PV-loop has a narrow shape, with high pressures, high volumes, and a small difference between end-diastolic and end-systolic volumes (Fig. 3, blue). This may be caused by the fact that the pressure is not slowly distributed among multiple vessel segments, given the limited number of arterial compartments included in this model.

MODEL 2: The BCG signal (Fig. 2, green) shows an improved amplitude difference between the J and L peaks.

However, it exhibits a non-standard pattern, with delayed peaks and a double peak instead of a single K peak. Model 2 has a more detailed description of the large arteries, with three aortic segments included explicitly (ascending aorta, aortic arch, thoracic aorta), followed by a group representing the abdominal aorta and iliac arteries (Fig. 4). This indicates that the more details are provided on the large arteries, the closer the simulated BCG waveform will be to the true BCG waveform. The PV-loop presents again a narrow shape (Fig. 3, green), with high pressures and high volumes. Hence, simply adding a more detailed description of the large arteries is not enough to improve on both the BCG and PV-loop.

MODEL 3: The amplitude difference between the J and L peaks in the BCG is more physiological (Fig. 2, cyan), even though a time delay is still present. This can be attributed to the fact that we used the same arterial circulation described in Model 1, which includes two arterial compartments, group 1 and group 2, with the addition of the cerebral circulation (Fig. 4). The PV-loop (Fig. 3, cyan) shows a remarkable improvement in pressure and volume values, which are now within the physiological ranges. Hence, adding cerebral circulation helps to better distribute volumes and pressures within the cardiovascular system.
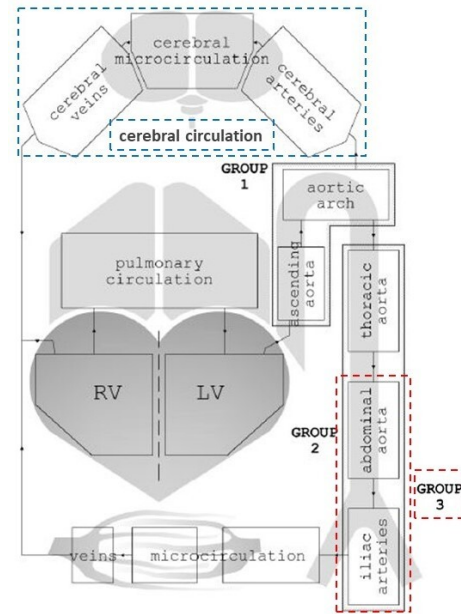

Figure 4. Cardiovascular model considering the aorta composed of two main groups, group 1 and 2 (black solid line), or the abdominal circulation and iliac arteries as group 3 (red dashed line), with a detailed cerebral description (blue block), for Model 3 and 4, respectively or without cerebral description for Model 1 and 2, respectively.

MODEL 4: The timing of the J peak (Fig. 2, purple) is consistent with that of Model 5. The K and L peaks are

not as pronounced, though, and are slightly delayed. The PV-loop (Fig. 3, purple) shows pressure and volume values within the physiological ranges and is similar to Model 5. This improvement can be attributed to the fact that the aortic segments are modeled explicitly, along with the presence of cerebral circulation.

MODEL 5: The BCG waveform (Fig. 2, black) is characterized by the typical I, J, K, and L peaks and valleys, and the LV-PV loop (fig. 3,black) is within physiological ranges. This result was achieved by including within the same closed-loop model a detailed description of the large arteries, from the ascending aorta to the iliac arteries, along with the presence of the cerebral circulation.

4.   Conclusions

The hierarchical analysis illustrated in this work highlights how not all closed-loop cardiovascular models are equally suitable for reconstructing the BCG waveform and the associated LV-PV loop. Clearly, all mathematical models have limitations, since they are based on simplifying assumptions that make them a tractable abstraction of the real complex world. Thus, the challenge is to understand what is the minimal complexity that is necessary to include in the model in order to capture the features of real waveforms that are deemed essential.

The important contribution of large arteries to the BCG is evidenced by the lack of any realistic peak when their description is not included (Model 0). This result is consistent with prior modeling work [3,4]. In addition, our comparative analysis shows that the cerebral circulation helps achieve better amplitude and timing of the BCG peaks, as well as more realistic LV-PV loops. This is an interesting finding that shows how the dynamics of blood pressure and volume distal from the major arteries does affect the BCG and LV-PV loop in a significant manner. This is a result of the fact that the cardiovascular system is a closed-loop network and, consequently, events happening anywhere in the system have repercussions along the network.

Computational modeling has the potential to significantly impact the understanding of cardiovascular physiology. For example, the level of cardiovascular detail of Model 5 allowed us to investigate the cardiovascular differences between men and women and how this is manifested in blood circulation, cardiovascular performances, and BCG signal [10]. Moreover, model parameters can be individualized for personalized cardiovascular monitoring through BCG signals [11]. While many challenges remain in translating this fundamental knowledge into practical technology, this work shows how modeling can help guide the design of sensing solutions whose signals can be interpreted on the basis of cardiovascular physiology.

References

[1] Starr I, Noordergraaf A. Ballistocardiography in cardiovascular research: Physical aspects of the circulation in health and disease. Lippincott, 1967.

[2] Noordergraaf A, Verdouw PD, Boom HB. The use of an analog computer in a circulation model. Prog Cardiovasc Dis 1963;5(5):419–439.

[3] Kim CS, Ober SL, McMurtry MS, Finegan BA, Inan OT, Mukkamala R, Hahn JO. Ballistocardiogram: Mechanism and potential for unobtrusive cardiovascular health monitoring. Sci Rep 2016;6:31297.

[4] Wiard RM, Kim HJ, Figueroa CA, Kovacs GT, Taylor CA, Giovangrandi L. Estimation of central aortic forces in the ballistocardiogram under rest and exercise conditions. In Conf Proc IEEE Eng Med Biol Soc. IEEE, 2009; 2831–2834.

[5] Guidoboni G, Sala L, Enayati M, Sacco R, Szopos M, Keller JM, Popescu M, Despins L, Huxley VH, Skubic M. Cardiovascular function and ballistocardiogram: a relationship interpreted via mathematical modeling. IEEE Trans Biomed Eng 2019;66(10):2906–2917.

[6] Zaid M, Sala L, Ivey JR, Tharp DL, Mueller CM, Thorne PK, Kelly SC, Silva KAS, Amin AR, Ruiz-Lozano P, et al. Mechanism-driven modeling to aid non-invasive monitoring of cardiac function via ballistocardiography. Front Med Tech 2022;4:788264.

[7] Avanzolini G, Barbini P, Cappello A, Cevenini G. CADCS simulation of the closed-loop cardiovascular system. Int J Biomed Comput 1988;22(1):39–49.

[8] Maceira AM, Prasad SK, Khan M, Pennell DJ. Normalized left ventricular systolic and diastolic function by steady state free precession cardiovascular magnetic resonance. J Magn Reson 2006;8(3):417–426.

[9] Hall JE, Hall ME. Guyton and Hall textbook of medical physiology e-Book. Elsevier Health Sciences, 2020.

[10] Zaid M, Sala L, Despins L, Heise D, Popescu M, Skubic M, Ahmad S, Emter CA, Huxley VH, Guidoboni G. Cardiovascular sex-differences: insights via physiology-based modeling and potential for noninvasive sensing via ballistocardiography. Front cardiovasc med 2023;10:1215958.

[11] Marazzi NM, Guidoboni G, Zaid M, Sala L, Ahmad S, Despins L, Popescu M, Skubic M, Keller J. Combining physiology-based modeling and evolutionary algorithms for personalized, noninvasive cardiovascular assessment based on electrocardiography and ballistocardiography. Front Physiol 2022;1953.

Address for correspondence:

Mohamed Zaid
University of Maine, 75 Long Rd, Orono, ME 04469
mohamed.zaid1@maine.edu